Accepted Manuscript

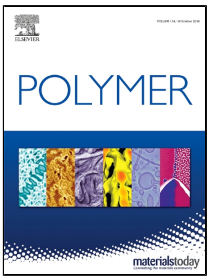

Novel anti-fouling PVDF-g-THFMA copolymer membrane fabricated via photoinduced Cu(II)-mediated reversible deactivation radical polymerization

Hongde Lei, Lu Liu, Lukuan Huang, Weixing Li, Weihong Xing

PII:	S0032-3861(18)30935-2
DOI:	10.1016/j.polymer.2018.10.019
Reference:	JPOL 20968
To appear in:	*Polymer*
Received Date:	05 May 2018
Accepted Date:	08 October 2018

Please cite this article as: Hongde Lei, Lu Liu, Lukuan Huang, Weixing Li, Weihong Xing, Novel anti-fouling PVDF-g-THFMA copolymer membrane fabricated via photoinduced Cu(II)-mediated reversible deactivation radical polymerization, *Polymer* (2018), doi: 10.1016/j.polymer.2018.10.019

Novel anti-fouling PVDF-g-THFMA copolymer membrane fabricated via photoinduced Cu(II)-mediated reversible deactivation radical polymerization

Hongde Lei, Lu Liu, Lukuan Huang, Weixing Li *, Weihong Xing

State Key Laboratory of Materials-Oriented Chemical Engineering, College of Chemical Engineering, Nanjing Tech University, Nanjing 210009, China

wxli@njtech.edu.cn

Abstract

In this study, we fabricated a novel anti-fouling poly(vinylidene fluoride) (PVDF) membrane using a novel amphiphilic copolymer of PVDF grafted with tetrahydrofurfuryl methacrylate (PVDF-g-THFMA). This copolymer was synthesized via photoinduced Cu(II)-mediated reversible deactivation radical polymerization. The amphiphilic copolymer was characterized by ^{1}H nuclear magnetic resonance and Fourier transform infrared spectroscopy. The morphology of the copolymer was examined using scanning electron microscopy. The permeability and hydrophilicity of the membranes were evaluated on the basis of their pure water flux and dynamic contact angles, respectively. The anti-fouling property of the membranes was evaluated by carrying out filtration using a bovine serum albumin (BSA) solution. The PVDF-g-THFMA copolymer membranes showed a pure flux of up to 293.9 L m^{-2} h^{-1} bar^{-1} and a molecular weight cut off of 39.5 kDa. After the filtration of the BSA solution, the

PVDF-g-THFMA copolymer membrane was washed with deionized water and the recovery ratio of the pure water flux reached a value of 89.1%. The modified membrane showed good filtration performance and anti-fouling property.

Key words: Poly(vinylidene fluoride) membrane; Poly(vinylidene fluoride) grafted with tetrahydrofurfuryl methacrylate; Photoinduced Cu(II)-mediated reversible deactivation radical polymerization; Hydrophilic modification; Anti-fouling property

1. Introduction

Among commercial polymers, poly(vinylidene fluoride) (PVDF) has received much attention as a membrane material owing to its excellent properties such as high mechanical strength, thermal stability, and outstanding chemical resistance to various organic solvents, acids, and bases [1–3]. However, the commercialization of PVDF membranes is limited. The surface energy of PVDF is very low, leading to the poor wettability and strong hydrophobic nature of PVDF membranes. Because of their hydrophobic nature, PVDF membranes are impressionable while treating aqueous solutions containing proteins. This increases the cost of operation and decreases the lifetime of PVDF membranes.

Many efforts have been made to improve the hydrophilicity of PVDF membranes. Coating a hydrophilic layer on the surface of PVDF membranes [4], grafting PVDF via various means such as ultraviolet (UV) photo irradiation, plasma, high-energy irradiation, and “living”/controlled polymerization, e.g. atom transfer radical polymerization (ATRP), and reverse atom transfer radical polymerization (RATRP) [5–

8], and introducing hydrophilic polymers [9], amphiphilic polymers, and inorganic nanoparticles into the membrane matrix have been proved to be effective in the modification of PVDF membranes [10–12].

Over the past few years, photochemically initiated ATRP, which offers the advantages of both ATRP and photopolymerization, has been studied extensively [13, 14]. Using this method, PVDF copolymers with a predetermined molecular weight and narrow molecular weight distribution can be synthesized. Compared to ATRP, photoinduced ATRP involves lower activation energy, faster reaction speed, and lower reaction temperature [15]. Yagci and co-workers developed the photoinduced Cu(II)-mediated reversible deactivation radical polymerization (RDRP) method. Cu(II) is of the utmost importance for the polymerization process in this method [16–18]. Over the past few years, photoinduced Cu(II)-mediated RDRP has received much attention and various modifications have been made to it [19]. In order to compensate for the unavoidable radical termination reactions in conventional ATRP, a high concentration of the Cu(I) catalyst is used. Cu(II)-mediated RDRP decreases the concentration of the copper catalyst used significantly without affecting the polymerization process. Compared to traditional reducing agents, light is an efficient and clean reducing agent for Cu(II). The light intensity reactor received can be changed by control the reaction equipment (the reactor was placed in it) size and polymerization time can be controlled through switching on or off light source. We can obtain polymer with certain grafting degree via control reaction equipment size and reaction time.[20]. The use of amphiphilic copolymers can improve the hydrophilicity of PVDF membranes in a

single step during the membrane fabrication itself [21, 22]. Owing to their self-assembling ability, these copolymers impart a uniform pore size, narrow pore size distribution, and high water flux to PVDF membranes. The strong interactions between the bulk polymer and hydrophobic chains of amphiphilic copolymers can effectively increase their compatibility and stability in the PVDF membrane matrix [23, 24]. Amphiphilic copolymers such as PVDF grafted with poly(methyl methacrylate) (PVDF-g-PMAA), PVDF grafted with poly(hydroxyethyl methacrylate) (PVDF-g-PHEMA), and PVDF grafted with poly(ethylene glycol) methyl ether methacrylate (PVDF-g-PEGMA) have been synthesized [25–27]. PVDF membranes using these amphiphilic copolymers as additives show excellent hydrophilicity and anti-fouling property. Recently, amphiphilic copolymers such as PVDF-co-chlorotrifluoroethylene)-graft-poly(methyl methacrylate) (P(VDF-co-CTFE)-g-PMMA) have been synthesized via photoinduced Cu(II)-mediated RDRP [28]. Motivated by these studies, we developed a PVDF amphiphilic copolymer membrane in this study. During the synthesis of PVDF amphiphilic copolymer membranes, a large number of hydrophilic segments are transferred to the membrane surface, which then self-assemble into regular pores. As a result, such membranes show good anti-fouling property and high flux.

In this study, we synthesized a novel amphiphilic copolymer of PVDF grafted with tetrahydrofurfuryl methacrylate (PVDF-g-THFMA) via photoinduced Cu(II)-mediated RDRP (a variation of ATRP) [29]. This copolymer was used to develop an anti-fouling ultrafiltration PVDF membrane via nonsolvent-induced phase separation. In this study,

THFMA was used to fabricate a PVDF grafting copolymer for the first time. The results showed that photoinduced Cu(II)-mediated RDRP is an efficient approach to modify PVDF membranes. To the best of our knowledge there have been no reports on modifying PVDF membranes using this approach. The morphology of the prepared membranes was investigated using a scanning electron microscope (SEM). The performance of the PVDF-g-THFMA copolymer membranes was evaluated on the basis of their pure water flux, molecular weight cut off (MWCO), rejection of bovine serum albumin (BSA), and protein filtration experiments.

2. Experimental

2.1. Materials

PVDF (Solef 1015, approximately 570,000–600,000 g/mol in Mw) was purchased from Solvay Specialty Polymers, Shanghai and was stored in a vacuum oven at 60 °C. THFMA, dextran with molecular weights of 10,000, 40,000, 70,000, and 500,000 Da and tris[2-(dimethylamino)ethyl]amine (Me_6-Tren) were purchased from Sigma-Aldrich, Shanghai. Copper(Ⅱ)chloride ($CuCl_2$) was supplied by Aladdin Industrial Corporation, Shanghai. 1-Methyl-2-pyrrolidinone (NMP) was supplied by Sinopharm Chemical Reagent Co. Ltd., Shanghai. BSA (67,000 Da) was purchased from Shanghai Huixing Biochemical Reagent Co. Ltd., China. Sodium chloride (NaCl) was supplied by Xilong Chemical Co. Ltd., China. Potassium chloride (KCl), disodium hydrogen phosphate dodecahydrate ($Na_2HPO_4 \cdot 12H_2O$), and potassium dihydrogen phosphate (KH_2PO_4) were purchased from Shanghai Lingfeng Chemical Reagent Co. Ltd., China.

Deionized (DI) water was obtained using a Milli-Q system (Millipore, US). All the solvents and chemicals used in this study were of reagent grade.

2.2. Synthesis and purification of PVDF-g-THFMA

First, 0.5 g PVDF and 0.01 g $CuCl_2$ were dissolved in 8 mL NMP in a self-made quartz vessel while stirring until the PVDF powder dissolved completely. Argon was used (1 h) to degas the dissolved oxygen in NMP. To the resulting solution, 0.03 mL Me_6-Tren and 4 mL THFMA were added. The sealed vessel was placed in a UV reactor and the reaction started under a UV radiation of 365 nm with stirring at ambient temperature. After 6 h, the reaction mixture was precipitated in DI water and was then washed thrice using ethyl alcohol. A soxhlet extractor was used to purify the product for 36 h to remove the unreacted THFMA monomer and THFMA homopolymer. The solvent used in the soxhlet extractor was a mixture of benzene and chloroform (v/v = 1/1). The purified product was dried in a vacuum oven at 60 °C. The grafting reaction is shown in Fig. 1.

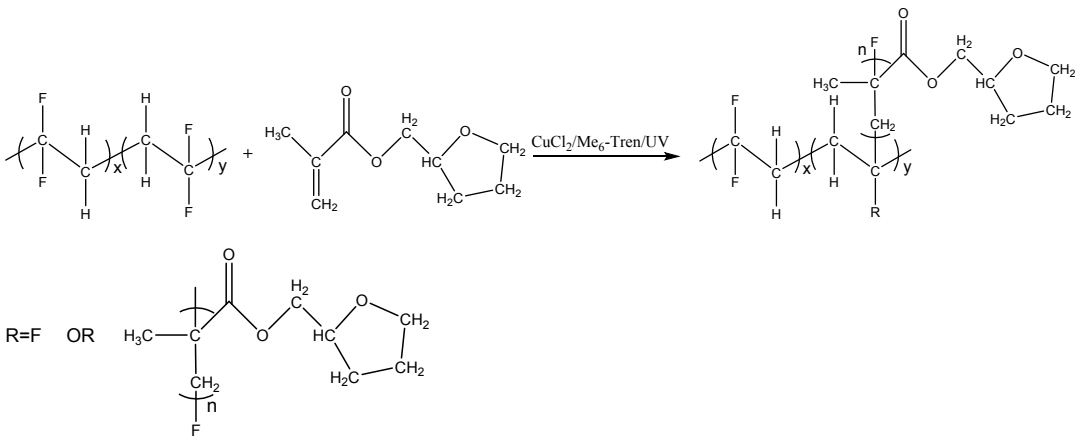

Fig. 1. Synthesis of the PVDF-g-THFMA copolymer.

2.3. Characterization of the PVDF-g-THFMA copolymer

^{1}H nuclear magnetic resonance (NMR) spectrum of the PVDF-g-THFMA copolymer was obtained using AVANCE AV-300 (Bruker, Switzerland). Dimethyl sulfoxide-d_6(DMSO-d_6) was used to dissolve the samples. The mole and weight fractions of THFMA in the amphiphilic PVDF-g-THFMA copolymer were calculated by using Eqs. (1) and (2), respectively [25]

$$\varphi_m(THFMA) = \frac{\frac{1}{9}(I_b + I_c + I_d)}{\frac{1}{9}(I_b + I_c + I_d) + \frac{1}{2}(I_{hh} + I_{ht})} \quad (1)$$

$$\varphi_w(THFMA) = \frac{\varphi_{m(THFMA)} \cdot M_{THFMA}}{\varphi_{m(THFMA)} \cdot M_{THFMA} + (1 - \varphi_{m(THFMA)}) \cdot M_{PVDF(unit)}} \quad (2)$$

where $\varphi_m(THFMA)$ and $\varphi_w(THFMA)$ denote the mole and weight fractions of THFMA in the PVDF-g-THFMA copolymer, respectively, I_x denotes the area under the corresponding peak in the NMR spectrum, M_{THFMA} and $M_{PVDF(unit)}$ denote the molecular weight of THFMA and PVDF units, respectively, and *hh* and *ht* refer to -$CF_2CH_2CH_2CF_2$- and -$CF_2CH_2CF_2CH_2$-, respectively.

The chemical composition of the PVDF-g-THFMA copolymer and pristine PVDF membranes was investigated using a Fourier transform infrared spectrometer (FTIR, Nicolet 8700, US).

2.4. Membrane preparation

The PVDF homopolymer and PVDF-g-THFMA copolymer membranes were fabricated via nonsolvent-induced phase separation with NMP as the solvent and DI

water as the nonsolvent coagulation bath. Before dissolving, PVDF and PVDF-g-THFMA were dried in a vacuum oven at 80 °C for 24 h in order to remove the absorbed water. PVDF and PVDF-g-THFMA were weighed accurately before adding them to the round-bottom flask containing NMP. The flask was heated and stirred in a water bath at 60 °C for 12 h to obtain a homogeneous casting solution and was then left in the water bath to degas fully. The dope solution was casted on a clean glass plate by a self-modified casting machine with a fixed gap of 150 μm at a speed of 3.0 $cm \cdot s^{-1}$. The nascent membrane was exposed to air for 20 s and was then immersed in DI water at room temperature (25 °C) and a relative humidity of around 60%. The resultant membranes were left immersed in DI water for 12 h to remove all the residual solvent, and DI water was replaced after every 4 h. Prior to the characterization, the membranes were preserved in DI water. The composition of the casting solutions is given in Table 1.

Table 1 Composition of the membrane casting solutions

Membrane code	NMP[a] (wt%)[b]	PVDF (wt%)	PVDF-g-THFMA (wt%)
P10	90	10	/
P15	85	15	/
P20	80	20	/
T10	90	/	10
T15	85	/	15
T20	80	/	20

[a]1-Methyl-2-pyrrolidinone

[b]weight percent.

2.5. Characterization of the membranes

2.5.1. Structure

The top surface and cross-section of the membranes were examined using a SEM (Hitachi S-4800, Japan). The samples were fractured in liquid nitrogen. The surface and cross-section of the membranes were coated with gold before carrying out the SEM analysis.

2.5.2. EDX measurement

In order to examine the distribution of THFMA segments in the PVDF-g-THFMA copolymer membrane, energy-dispersive X-ray spectroscopy (EDX) (equipped on SEM) (S-4800, Hitachi, Japan) was used. The distribution of elements such as oxygen, carbon, and fluorine in the entire cross-section of the membrane was examined. The test samples were prepared in the presence of liquid nitrogen.

2.5.3. Dynamic contact angle measurement

The hydrophilicity of the surface of the membranes was evaluated on the basis of their dynamic contact angles measured using a contact angle meter (DSA 100, Kruss, Germany). The contact angles were measured using a 3.0–4.0 μL droplet of DI water at ambient temperature. The average of at least five observations (five different locations of each membrane) was used.

2.5.4. Filtration performance

The pure water flux (J_{w1}) of the membranes was measured using a dead-end filtration device (Amicon 8400, Millipore, US) with an effective membrane area of

4.1×10^{-4} m^2. The working pressure was controlled using a nitrogen gas tank and the measurements were carried out at ambient temperature. DI water was used as the filtration media. First, the membranes were compacted under a trans-membrane pressure of 1.5 bar for 20 min. Once a steady flux was attained, the measurements were carried out under a trans-membrane pressure of 1.0 bar. The pure water flux was calculated using Eq. (3)

$$J_{w1} = \frac{V}{A\Delta t} \tag{3}$$

where V is the volume of DI water (L), A is the effective area of the membranes (m^2), and Δt is the filtration time (h).

2.2.5. MWCO

The MWCO of the membranes was measured using a cross-flow apparatus. An aqueous solution of dextran with different molecular weights (10,000, 40,000, 70,000, and 500,000 Da) was used as the feed solution. The dextran solution was circulated in the apparatus for 1.0 h at a pressure of 1.0 bar and room temperature. The feed and permeate solutions were analysed by gel permeation chromatography (GPC, Waters, USA). The molecular weight of dextran which was retained over 90% was considered as the MWCO.

2.5.6. Fouling resistance

The anti-fouling property of the modified membrane was evaluated by carrying out permeation experiments with BSA as a model pollutant. The measurement device used

here was the same as that used for the measurement of MWCO. The operation was similar to the pure water flux measurement. DI water was replaced by a phosphate-buffered saline (PBS) solution (pH = 7.4) containing BSA. The PBS solution was an aqueous solution containing NaCl (8.0 g), KCl (0.2 g), $Na_2HPO_4 \cdot 12H_2O$ (3.63 g), KH_2PO_4 (0.24 g), and DI water (1 L). The BSA solution flux was recorded after every 10 min for the first 40 min and after every 15 min for the remaining time. The test time was 120 min. After the permeation of the BSA solution, the membranes were flushed with DI water thoroughly. The recovered pure water flux (J_{w2}) was measured again. The water flux recovery ratio (*FRR*) was calculated by Eq. (4).

$$FRR(\%) = \frac{J_{w2}}{J_{w1}} \times 100 \quad (4)$$

BSA rejection is a measure of the separation property of a membrane. The BSA concentrations in the feed and permeate sides were measured by a UV-vis spectrophotometer (UV-6000, Shanghai Yuanyi Apparatus Co., Ltd, China.) at 280 nm. The BSA rejection (*R*) of the membranes was calculated by Eq. (5)

$$R(\%) = (1 - \frac{C_p}{C_f}) \times 100 \quad (5)$$

where C_p(g/L) and C_f(g/L) are the concentrations of the permeate and feed BSA solution, respectively.

3. Results and discussion

3.1. NMR characterization

The structures of PVDF and PVDF-g-THFMA were verified by ^{1}H NMR. Figure 2

shows a series of characteristic peaks corresponding to the protons in THFMA (absent in the case of PVDF), confirming the presence of THFMA in the PVDF-g-THFMA copolymer. PVDF showed peaks at 2.25 and 2.89 ppm corresponding to the -$CF_2CH_2CH_2CF_2$- (*hh*) and -$CF_2CH_2CF_2CH_2$- (*ht*) groups, respectively. Peak b corresponds to the methylene group. Peaks c and d can be attributed to the oxygenated heterocyclic ring in tetrahydrofurfuryl methacrylate. The mole (3.1%) and weight fractions (7.7%) of THFMA in the PVDF-g-THFMA copolymer were calculated using Eqs. (1) and (2), respectively.

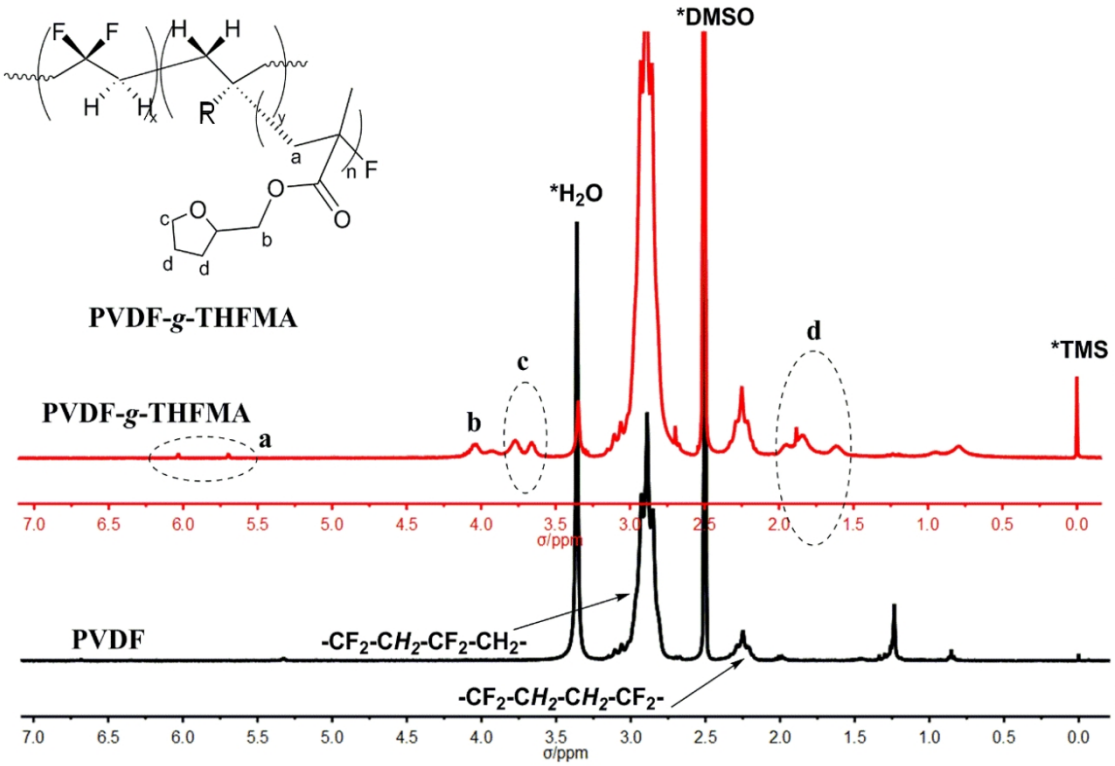

Fig. 2. ^{1}H NMR spectra of PVDF and PVDF-g-THFMA.

3.2. FTIR analysis

The grafting of THFMA monomer on PVDF was further confirmed by carrying out the FTIR analysis of the membranes. In Fig. 3, the peaks at 2939 and 2877 cm^{-1} correspond to the stretching vibration of -CH in $-CH_3$ and the peak at 1731 cm^{-1} corresponds to the stretching vibration of -C=O in -COO-. The FTIR results confirm that the PVDF-g-THFMA copolymer membrane was synthesized successfully.

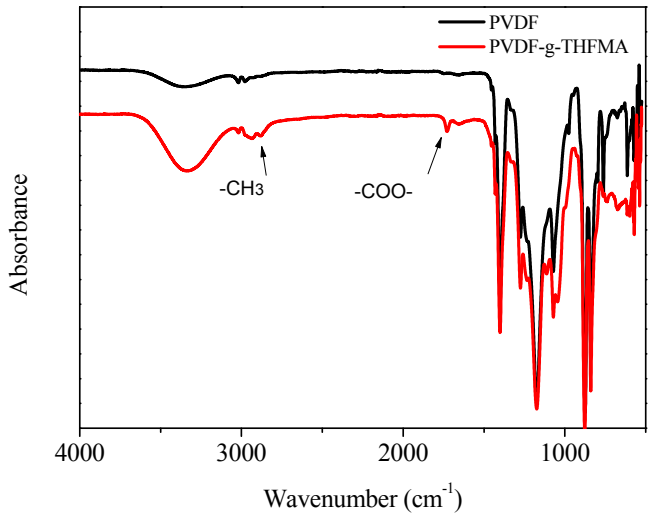

Fig. 3. FTIR spectra of PVDF and PVDF-g-THFMA.

3.3. Membrane characterization

3.3.1. Morphology of the membranes

In order to investigate the effect of THFMA on the microstructure of the membranes, their microstructures were observed by SEM. Figure 4 shows that the P20-C PVDF membrane contained a large number of finger-like pores, while the T20-C PVDF-g-THFMA copolymer membrane contained a large number of voids. When the concentration of the casting solution was low, both the PVDF homopolymer (P10-C) and PVDF-g-THFMA copolymer (T10-C) membranes showed a macrovoid structure. During phase inversion, hydrophilic polymers have a shorter phase inversion time than

hydrophobic polymers, thus forming more finger-like holes [30]. Since the oxygen atoms in THFMA could easily form hydrogen bonds with the hydrogen atoms in water molecules, the PVDF-g-THFMA copolymer membranes were more hydrophilic than the PVDF membranes. It can be speculated that the hydrophilic THFMA segments migrated to the surface of the membrane during phase inversion, and hence self-assembled, leading to the formation of a large number of uniform pores on the membrane surface. The hydrophilic THFMA segments repelled each other during their migration to the top surface of the membrane, leading to the formation of a large number of uniform pores. Liu reported that the self-assembly of amphiphilic block copolymers such as poly(styrene-b-4-vinylpyridine) (PS4VP) results in the formation of uniform pores [31]. It can be observed from Fig. 4 that the pores in the T10-S PVDF-g-THFMA copolymer membrane were more homogeneous than those in the P10-S PVDF membrane.

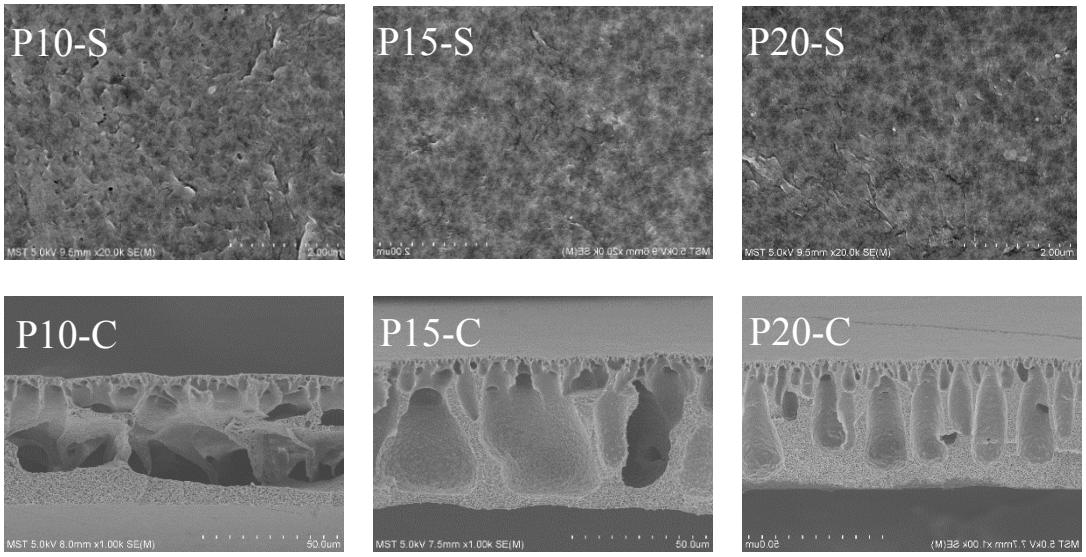

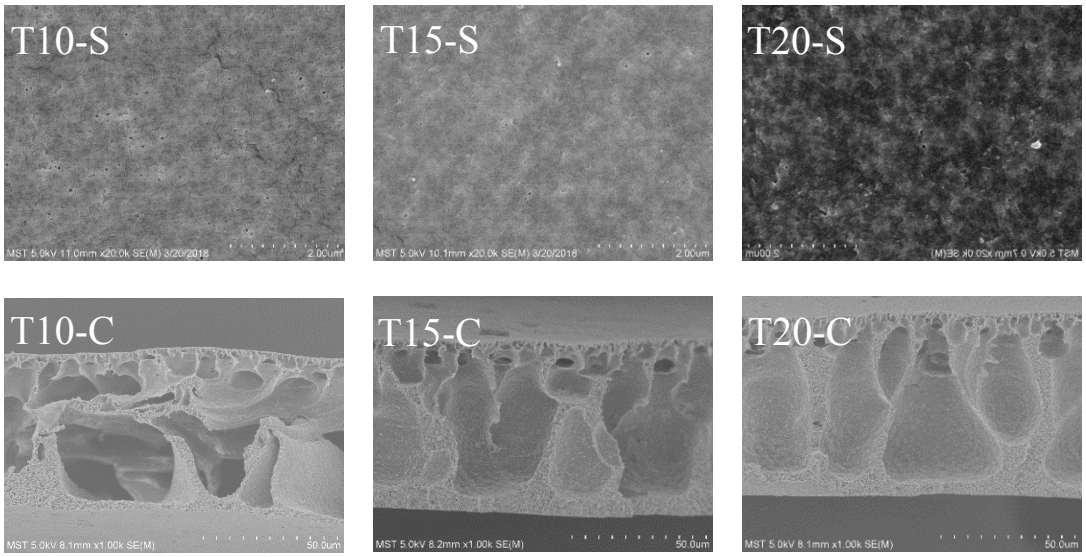

Fig. 4. Microstructure of the top surface and cross-section of the PVDF (P10, P15, P20) and PVDF-g-THFMA copolymer (T10, T15, T20) membranes with coagulation at room temperature (20 ºC) and a relative humidity of around 60%. S and C refer to the top surface and cross-section of the membranes, respectively.

3.3.2 EDX analysis

The distribution of oxygen atoms in the PVDF-g-THFMA copolymer membrane was analysed by EDX equipped on SEM. Figure 5 shows that oxygen atoms were distributed more on the surface of the membrane, while carbon and fluorine atoms were evenly distributed throughout the cross-section of the membrane. This suggests that the THFMA segments migrated to the top surface of the membrane during the phase inversion process. These results are consistent with the SEM results. The presence of THFMA segments on the top surface of the membrane resulted in the formation of a large number of uniform pores. The cross-section of the PVDF-g-THFMA copolymer membrane showed a looser structure and had a large number of macrovoids as

compared to the PVDF membrane.

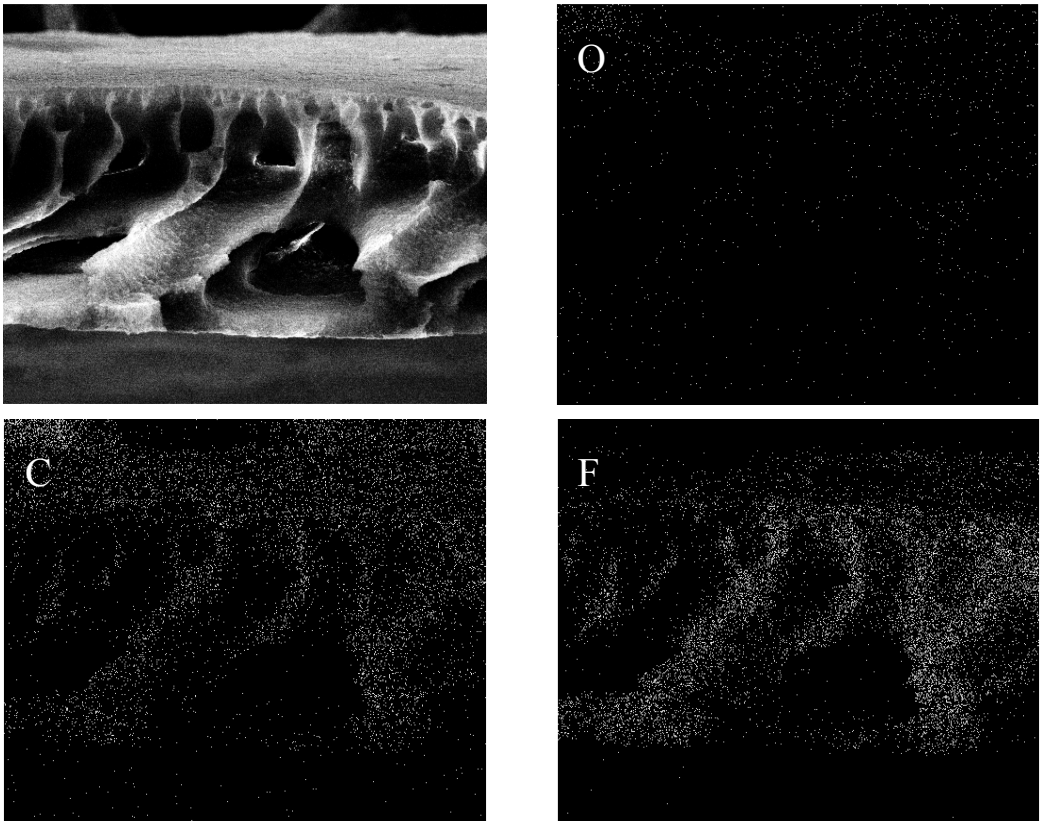

Fig. 5. Distribution of O, C, and F atoms in the cross-section of the PVDF-g-THFMA copolymer membrane.

3.3.3. Dynamic contact angle measurement

The hydrophilicity of the PVDF and PVDF-g-THFMA copolymer membrane surfaces was evaluated by measuring their dynamic contact angles. Figure 6 shows that the initial contact angle of the PVDF-g-THFMA copolymer membrane was smaller than that of the PVDF membrane at different casting solution concentrations. After 3 min, the PVDF-g-THFMA copolymer membrane showed a large decrease in the contact angle as compared to the PVDF membrane. This indicates that the surface

contact angle of the PVDF-g-THFMA copolymer membrane decreased at a higher rate. Hence, it can be stated that the presence of THFMA segments improves the hydrophilicity of PVDF membranes. This can be attributed to the fact that hydrophilic THFMA segments migrate to the membrane surface. These results were consistent with the EDX results (Section 3.3.2). During phase inversion, the THFMA segments migrated to the membrane surface, which made its distribution on the membrane top surface redundant. Oxygen atoms in the THFMA segments easily hydrated with water molecules, thus improving the hydrophilicity of the PVDF-g-THFMA copolymer membranes.

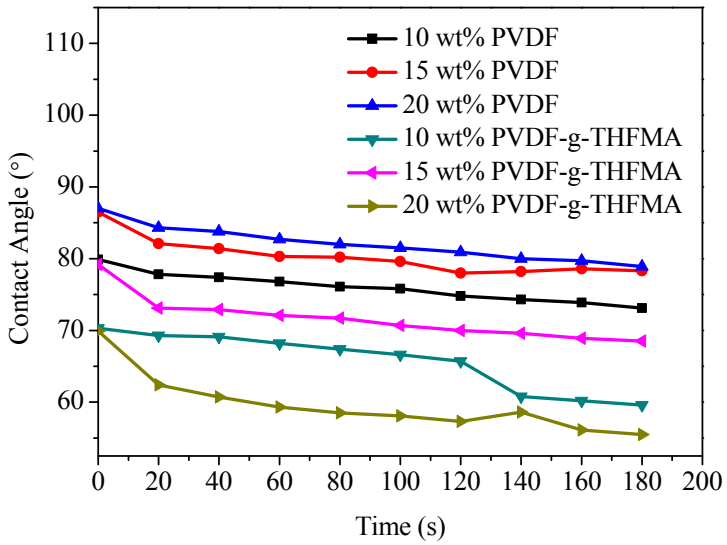

Fig. 6. Dynamic contact angles of the PVDF and PVDF-g-THFMA copolymer membranes.

3.3.4. Filtration performance

Pure water flux and MWCO are important parameters for analysing the permeation and rejection properties of a membrane. As can be observed from Table 2, at the same

casting solution ratio, the modified membrane showed a higher pure water flux than the PVDF membrane. The pure water fluxes of the T20 and T15 PVDF-g-THFMA copolymer membranes were found to be 40.7 and 167.5 L m^{-2} h^{-1} bar^{-1}, respectively, which are 6.3 and 6.4 times higher than those of the P20 and P15 PVDF membranes, respectively. The pure water flux of T10 was found to be 293.9 L m^{-2} h^{-1} bar^{-1}, which is significantly higher than that of the P10 PVDF membrane (130.8 L m^{-2} h^{-1} bar^{-1}). The PVDF-g-THFMA copolymer membranes had a large number of finger-like pores, resulting in a reduced mass transfer resistance of water through them. Since the top surface of the PVDF-g-THFMA copolymer membranes contained a large number of pores, their pure water flux was significantly higher than that of the PVDF membranes. The contact angle measurement results (Section 3.3.3) showed that after 3 min of testing, the contact angles of P10, P15, and P20 were 73.1°, 78.3°, and 78.9°, respectively, while those of T10, T15, and T20 were 59.6°, 68.5°, and 55.5°, respectively. It was found that the surface of the modified membranes was more hydrophilic and wetted easily. One of the reasons for their higher pure water flux was the formation of a hydration layer on their surface

Because of the self-assembly of THFMA chains during the formation of the PVDF-g-THFMA copolymer membrane, a large number of uniform pores were formed on its surface. The MWCO of the modified membrane was significantly lower than that of the PVDF membrane. The MWCO of the P15 and P20 PVDF homopolymer membranes was found to be 23.6 and 14.1 kDa, respectively. On the other hand, the MWCO of the T15 and T20 PVDF-g-THFMA copolymer membranes was found to be

12.2 and 11.6 kDa, respectively.

We also compared the PVDF-g-THFMA copolymer membrane developed in this study with the PEGMA- [32], POEM- [33], PHEMA- [27], PACMO- [34], MABS-modified [35] membranes reported previously. As can be observed from Fig. 7, the BSA rejection and pure water flux of the PVDF-g-THFMA copolymer membrane were higher than those of the membranes modified with POEM and PEGMA, which are commonly used hydrophilic monomers. The rejection rate of the PVDF-g-THFMA copolymer membranes (88.2%) was lower than that of the PVDF membranes modified with PACMO and MABS. However, the modified membranes developed in this study showed a high pure water flux (reaching up to 293.9 L m^{-2} h^{-1} bar^{-1}).

Table 2 Pure water flux and MWCO of the PVDF and PVDF-g-THFMA copolymer membranes

Membrane code	Pure water flux (Lm^{-2} h^{-1} bar^{-1})	MWCO[a] (kDa)
P10	130.8±33.6	45.6±6.5
P15	26.2±0.3	23.6±3.5
P20	6.5±1.5	14.1±4.1
T10	293.9±114.7	39.5±5.4
T15	167.5±16.0	12.2±4.4
T20	40.7±2.1	11.6±2.0

[a]molecular weight cut off.

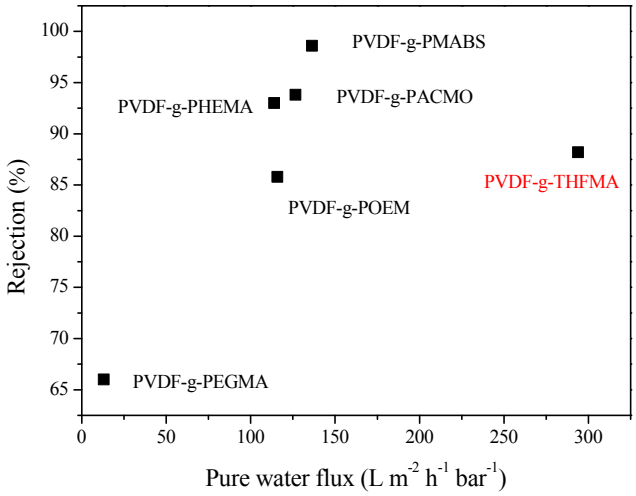

Fig. 7. Comparison of the PVDF-g-THFMA copolymer membrane and other amphiphilic copolymer-modified membranes. PVDF-g-PEGMA is PVDF grafted with poly(ethylene glycol) methyl ether methacrylate (PEGMA), PVDF-g-POEM is PVDF grafted with poly(oxyethylene methacrylate) (POEM), PVDF-g-PHEMA is PVDF grafted with poly(hydroxyethyl methacrylate) (PHEMA), PVDF-g-PACMO is PVDF grafted with polyacryloylmorpholine (PACMO), and PVDF-g-PMABS is PVDF grafted with 4-methacrylamidobenzenesulfonic acid (MABS).

3.3.5. Anti-fouling performance

Sodium alginate (SA), humic acid (HA), and BSA are commonly used to evaluate the fouling resistance of membranes. In this study, we used a BSA solution to evaluate the anti-fouling property of the membranes. Table 3 gives the BSA rejection and pure water flux recovery ratio of the membranes after washing with DI water. It can be observed from the table that the BSA rejection of the PVDF-g-THFMA copolymer membrane was higher than that of the PVDF membrane. The BSA rejection for the T15

PVDF-g-THFMA copolymer membrane was found to be 91.3%, while that for P15 was 87.3%. The BSA rejection of the T10 and T20 PVDF-g-THFMA copolymer membranes was found to be 88.2% and 85.4%, respectively, which is higher than that obtained for the P10 (74.5%) and P20 (83.0%) PVDF homopolymer membranes . The pure water flux recovery ratios were measured after cleaning the membranes with fresh water. The recovery ratios of the PVDF-g-THFMA copolymer membranes (minimum being 84.5%) were higher than those of the PVDF homopolymer membranes (maximum being 77.1%).

To investigate the fouling resistance of the membranes, their BSA filtration tests were conducted. The results are shown in Fig. 8. It can be seen from the figure that the PVDF-g-THFMA copolymer membranes showed a higher BSA stable flux than the corresponding PVDF membranes. The stable flux of the T10 and T15 PVDF-g-THFMA copolymer membranes was found to be 90.3 and 37.9 L m^{-2} h^{-1} bar^{-1}, respectively, while that of the P10 and P15 PVDF membranes P10 and P15 was found to be 55.2 and 10.5 L m^{-2} h^{-1} bar^{-1}, respectively. These results suggest that the anti-fouling ability of PVDF membranes can be significantly improved by grafting THFMA segments onto them.

Table 3 BSA rejection and recovery ratio of pure water flux for the PVDF and PVDF-g-THFMA copolymer membranes

Membrane code	BSA rejection (%)	Recovery ratio (%)
P10	74.5±1.6	75.6±2.5
P15	87.3±2.2	73.8±3.6
P20	83.0±3.4	77.1±3.4

T10	88.2±4.3	87.6±2.8
T15	91.3±3.5	89.1±3.1
T20	85.4±2.3	84.5±3.9

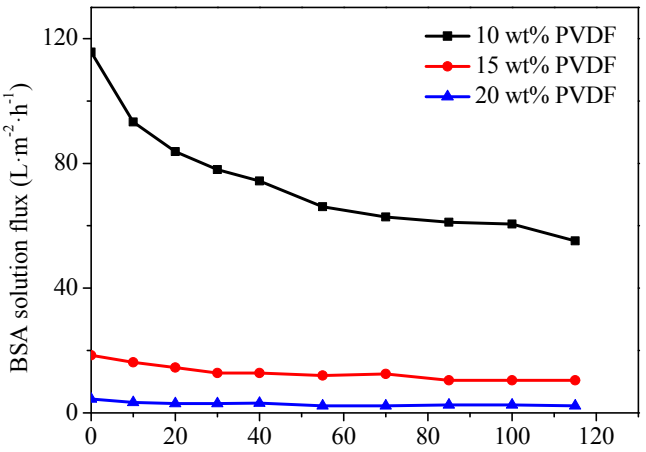

(a)

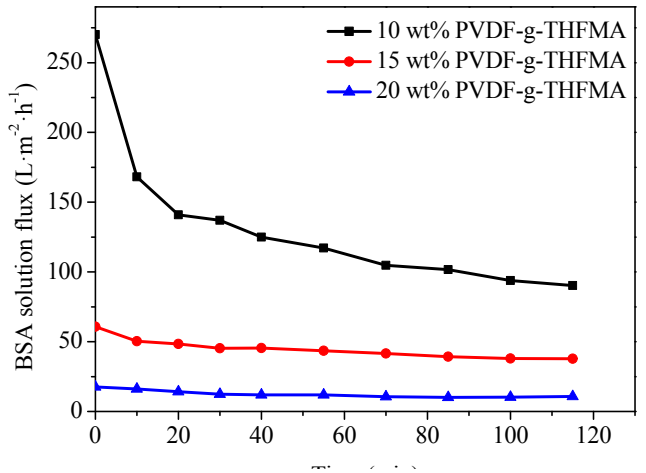

(b)

Fig. 8. BSA solution flux of the (a) PVDF and (b) PVDF-g-THFMA copolymer membranes.

4. Conclusion

A novel amphiphilic copolymer of PVDF-g-THFMA was synthesized and was then used to fabricate a PVDF-g-THFMA copolymer membrane. Photoinduced Cu(II)-

mediated RDRP was employed for the first time to synthesize the copolymer. The results showed that the PVDF-g-THFMA copolymer membrane exhibited outstanding hydrophilicity and resistance to contamination. The contact angle of the modified membrane reached to 55.5° after 3 min of testing. The maximum pure water flux of the PVDF-g-THFMA copolymer membrane reached up to 293.9 L m^{-2} h^{-1} bar^{-1}, and the recovery ratio of the pure water flux after BSA filtration reached up to 89.1%, which was much higher than that of the pristine PVDF membrane.

Acknowledgements

The authors gratefully acknowledge the financial support from National Natural Science Foundation of China (No. 21576132), National Key R&D Program of China (2017YFD0400402), and Yanhu plan of Qinhai (Q-SYS-201516-KF-01).

References

[1] K. Yoon, B.S. Hsiao, B. Chu, High flux ultrafiltration nanofibrous membranes based on polyacrylonitrile electrospun scaffolds and crosslinked polyvinyl alcohol coating, J. Membr. Sci. 338 (2009) 145-152.

[2] W. Lang, Z. Xu, H. Yang, W. Tong, Preparation and characterization of PVDF-PFSA blend hollow fiber UF membrane, J. Membr. Sci.288 (2007) 123-131.

[3] A. Figoli, S. Simone, A. Criscuoli, S.A. AL-Jlil, F.S. Al Shabouna, H.S. Al-Romaih, E. Di Nicolò, O.A. Al-Harbi, E. Drioli, Hollow fibers for seawater desalination from blends of PVDF with different molecular weights: Morphology, properties and VMD performance, Polymer. 55 (2014) 1296-1306.

[4] K. Ko, Y. Yu, M. Kim, J. Kweon, H. Chung, Improvement in fouling resistance of silver-graphene oxide coated polyvinylidene fluoride membrane prepared by pressurized filtration, Sep. Purif. Technol. 194 (2018) 161-169.

[5] N. Hilal, V. Kochkodan, L. Al-Khatib, T. Levadna, Surface modified polymeric membranes to reduce (bio)fouling: a microbiological study using E. coli, Desalination. 167 (2004) 293-300.

[6] P. Wang, K.L. Tan, E.T. Kang, K.G. Neoh, Plasma-induced immobilization of poly(ethylene glycol) onto poly(vinylidene fluoride) microporous membrane, J. Membr. Sci. 195 (2002) 103-114.

[7] M. Ejaz, S. Yamamoto, Y. Tsujii, T. Fukuda, Fabrication of patterned high-density polymer

graft surfaces. 1. Amplification of phase-separated morphology of organosilane blend monolayer by surface-initiated atom transfer radical polymerization,Macromolecules. 35 (2002) 1412-1418.

[8] F. Liu, B. Zhu, Y. Xu, Improving the hydrophilicity of poly(vinylidene fluoride) porous membranes by electron beam initiated surface grafting of AA/SSS binary monomers, Appl. Surf. Sci. 253 (2006) 2096-2101.

[9] J.M.N.A. Martin Masuelli, SPC/PVDF membranes for emulsified oily wastewater treatment, J. Membr. Sci.326 (2009) 688-693.

[10] S. Wang, T. Li, C. Chen, S. Chen, B. Liu, J. Crittenden, Non-woven PET fabric reinforced and enhanced the performance of ultrafiltration membranes composed of PVDF blended with PVDF-g-PEGMA for industrial applications, Appl. Surf. Sci. 435 (2018) 1072-1079.

[11] J. Zhang, Z. Wang, Q. Wang, C. Pan, Z. Wu, Comparison of antifouling behaviours of modified PVDF membranes by TiO_2 sols with different nanoparticle size: Implications of casting solution stability, J. Membr. Sci. 525 (2017) 378-386.

[12] Y. Lu, S.L. Yu, B.X. Chai, Preparation of poly(vinylidene fluoride)(PVDF) ultrafiltration membrane modified by nano-sized alumina (Al_2O_3) and its antifouling research, Polymer. 46 (2005) 7701-7706.

[13] K.S.J.B. Dominik Konkolewicz, Visible light and sunlight photoinduced ATRP with ppm of Cu catalyst. Macroletters. 1 (2012) 1219-1223.

[14] J.M.E.A. Ková, Photochemically mediated atom transfer radical polymerization of methyl methacrylate using ppm amounts of catalyst, Macromolecules. 45 (2012) 5859-5865.

[15] S.J.A.N. Yusuf Yagci, Photoinitiated polymerization:Advances, challenges, and opportunities, Macromolecules. 43 (2010) 6245-6260.

[16] M.A. Tasdelen, M. Uygun, Y. Yagci, Photoinduced controlled radical polymerization, Macromol. Rapid. Commun.211 (2011) 2271-2275.

[17] M.A. Tasdelen, M. Uygun, Y. Yagci, Studies on photoinduced ATRP in the presence of photoinitiator, Macromol. Chem. Phys. 212 (2011) 2036-2042.

[18] M.A. Tasdelen, M. Çiftci, M. Uygun, Y. Yagci, Possibilities for Photoinduced controlled radical polymerizations, Acs. Sym. Ser. 1100 (2012) 59-72.

[19] B. Wenn, M. Conradi, A.D. Carreiras, D.M. Haddleton, T. Junkers, Photo-induced copper-mediated polymerization of methyl acrylate in continuous flow reactors, Polym. Chem. 5 (2014) 3053-3060.

[20] X. Hu, N. Zhu, Z. Fang, Z. Li, K. Guo, Continuous flow copper-mediated reversible deactivation radical polymerizations, Eur. Polym. J. 80 (2016) 177-185.

[21] F. Liu, Y. Xu, B. Zhu, L. Zhu, F. Zhang, Preparation of hydrophilic and fouling resistant poly(vinylidene fluoride) hollow fiber membranes, J. Membr. Sci. 345 (2009) 331-339.

[22] Y. Zhao, Y. Qian, B. Zhu, Y. Xu, Modification of porous poly(vinylidene fluoride) membrane using amphiphilic polymers with different structures in phase inversion process, J. Membr. Sci. 310 (2008) 567-576.

[23] B. Reining, H. Keul, H. H Cker, Amphiphilic block copolymers comprising poly(ethylene oxide) and poly(styrene) blocks: synthesis and surface morphology, Polymer. 43 (2002) 7145-7154.

[24] B.F.W.A. Jian-Jun Qin A, A high flux ultrafiltration membrane spun from PSU/PVP(K90)/DMF/1,2-propanediol, J. Membr. Sci. 211 (2003) 139-147.

[25] B. Liu, C. Chen, T. Li, J. Crittenden, Y. Chen, High performance ultrafiltration membrane composed of PVDF blended with its derivative copolymer PVDF-g-PEGMA, J. Membr. Sci. 445 (2013) 66-75.

[26] J.F. Hester, P. Banerjee, Y.Y. Won, A. Akthakul, M.H. Acar, A.M. Mayes, ATRP of amphiphilic graft copolymers based on PVDF and their use as membrane additives, Macromolecules. 35 (2002) 7652-7661.

[27] S. Yan, Z. Wang, X. Gao, C. Gao, Antifouling PVDF ultrafiltration membranes incorporating PVDF-g-PHEMA additive via atom transfer radical graft polymerizations, J. Membr. Sci. 413-414 (2012) 38-47.

[28] X. Hu, G. Cui, Y. Zhang, N. Zhu, K. Guo, Copper(II) photoinduced graft modification of P(VDF-co-CTFE), Eur. Polym. J. 100 (2018) 228-232.

[29] C.A. Smolders, A.J. Reuvers, R.M. Boom, I.M. Wienk. Microstructures in phase-inversion membranes. Part 1. Formation of macrovoids, J. Membr. Sci. 73 (1992) 259-275.

[30] H. Strathmann, K. Kock, P. Amar, R.W. Baker, The formation mechanism of asymmetric membranes, Desalination. 16 (1975) 179-203.

[31] Y. Liu, T. Liu, Y. Su, H. Yuan, T. Hayakawa, X. Wang. Fabrication of a novel PS4VP/PVDF dual-layer hollow fiber ultrafiltration membrane, J. Membr. Sci. 506 (2016) 1-10.

[32] N.A. Hashim, F. Liu, K. Li, A simplified method for preparation of hydrophilic PVDF membranes from an amphiphilic graft copolymer, J. Membr. Sci. 345 (2009) 134-141.

[33] M.R.M. Abed, S.C. Kumbharkar, A.M. Groth, K. Li, Economical production of PVDF-g-POEM for use as a blend in preparation of PVDF based hydrophilic hollow fibre membranes, Sep. Purif. Technol. 106 (2013) 47-55.

[34] J. Liu, X. Shen, Y. Zhao, L. Chen, Acryloylmorpholine-grafted PVDF membrane with improved protein fouling resistance, Ind. Eng. Chem. Res. 52 (2013) 18392-18400.

[35] F. Chen, X. Shi, X. Chen, W. Chen,c,Preparation and characterization of amphiphilic copolymer PVDF-g-PMABS and its application in improving hydrophilicity and protein fouling resistance of PVDF membrane, Appl. Surf. Sci.427(2018)787–797.

- A new amphiphilic copolymer was synthesized.
- A novel PVDF-g-THFMA copolymer membrane with anti-fouling property was prepared by nonsolvent induced phase separation.
- Hydrophilic modification of PVDF membrane via photoinduced Cu(II)-mediated RDRP for the first time.

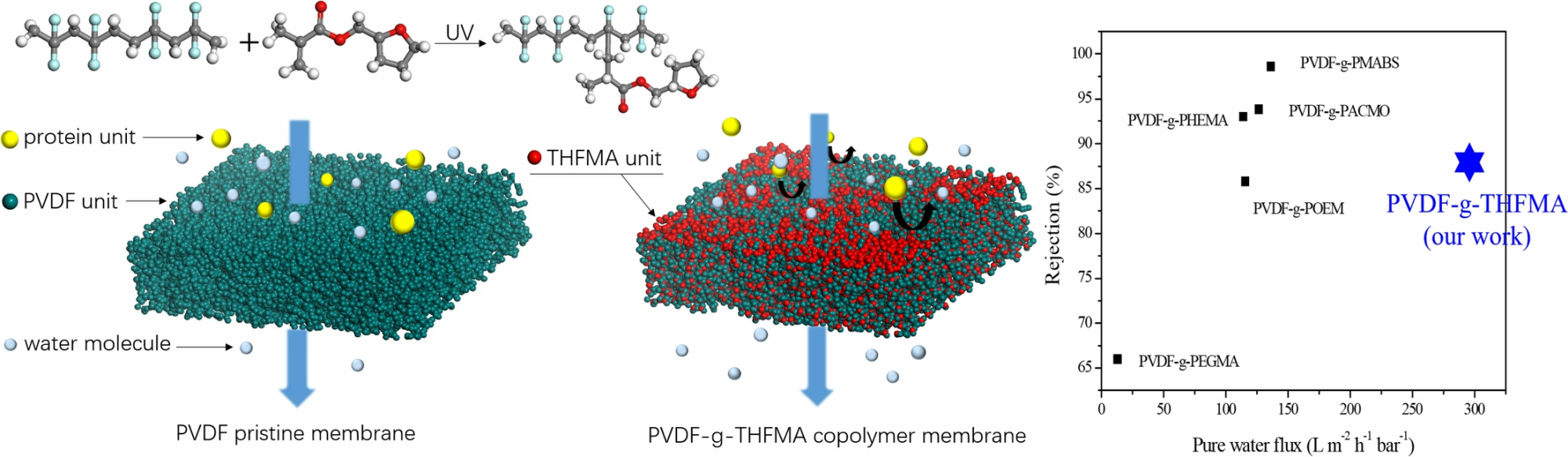
UV
protein unit
PVDF unit
water molecule
THFMA unit
PVDF pristine membrane
PVDF-g-THFMA copolymer membrane
PVDF-g-PMABS
PVDF-g-PHEMA
PVDF-g-PACMO
PVDF-g-POEM
PVDF-g-THFMA
(our work)
PVDF-g-PEGMA
Rejection (%)
Pure water flux (L m-2 h-1 bar-1)
100
95
90
85
80
75
70
65
0
50
100
150
200
250
300